Orientation correlation of p-nitroaniline molecules in acetone solution observed by hyper-Rayleigh scattering

David P. Shelton
Department of Physics and Astronomy, University of Nevada, Las Vegas, Nevada 89154-4002, USA

(Received 11 November 2012; accepted 14 January 2013; published online 1 February 2013)

Measurements of the polarization dependence of hyper-Rayleigh scattering (HRS) by solutions of p-nitroaniline (PNA) in acetone-d6 were used to study molecular orientation correlations. The HRS observations were analyzed in terms of short range direct dipole-dipole correlations between the PNA molecules, a long range transverse polar mode for the PNA molecules, and a long range ion-induced longitudinal polar mode. The conclusion that long range correlations are present is opposite to that in previous work, due to previous neglect of the ion-induced contribution. Depolarized HRS not explained by local correlations appears above 0.1 M PNA concentration, and analysis of the HRS observations indicates strong orientation correlations with a range of 10 nm for the PNA molecules.
 [http://dx.doi.org/10.1063/1.4789480]

I. INTRODUCTION

Hyper-Rayleigh scattering (HRS) is a second harmonic light scattering process widely used to measure the first hyperpolarizability β of molecules in solution.[1] It is usually assumed that the orientations of dissolved chromophores in dilute solution are uncorrelated and random so that the HRS intensity is proportional to the orientational average $\langle\beta^2\rangle$ for individual chromophores.[2,3] However, HRS is sensitive to intermolecular correlations and interactions[2–6] and several recent HRS experiments have observed such effects in neat liquids[6–8] and solutions.[9–11] Intermolecular interactions and correlations change the observed intensity, spectrum, and polarization dependence of the HRS light.

A recent HRS study used solutions of p-nitroaniline (PNA) in acetone to probe the range of intermolecular correlations.[11] In that experiment the HRS signal of the solution was dominated by HRS from the highly nonlinear chromophore (PNA), correlations between the PNA probe molecules resulted in changes in the polarization dependence of the observed HRS signal, and the distance between the probe molecules was adjusted by varying the PNA concentration. The conclusion of the study is that the intermolecular correlations are short range.[11] This conclusion is consistent with the usual view of liquids, but is opposite to the conclusion of other recent HRS studies which find long range correlations in nitrobenzene-benzene solutions[10] and a variety of neat liquids.[8]

The present work repeats the HRS experiments of Chan and Wong with PNA-acetone solutions,[11] but reaches the opposite conclusion. The experimental observations in the present and the previous work agree, except that the present work also includes observations of the effect of dissolved ions. The additional observations show that the previous analysis is invalid, and the revised analysis leads to the opposite conclusion.

II. EXPERIMENT AND RESULTS

The present HRS measurements were made at laser wavelength $\lambda_0 = 1064$ nm with linear polarized light, at or near the 90° scattering angle, using previously described apparatus and techniques.[7,8,10,12,13] The usual 90° scattering configurations with incident and scattered light polarized either perpendicular or parallel to the horizontal scattering plane are denoted VV, HV, VH, and HH, where V denotes vertical polarization, H denotes horizontal polarization, and the first and second letters refer to the incident and scattered light, respectively. The HRS intensity I_{VV} and the intensity ratios I_{VV}/I_{HV} and I_{HV}/I_{VH} were measured. The ratio I_{HV}/I_{VH} is the indicator for long range orientation correlations.[8,10,14] The spectral band for the detected HRS light was determined by a filter centered at 532 nm, with either 60 cm^{-1} or 0.3 cm^{-1} spectral bandwidth ($\Delta\nu$, full width at half maximum transmission). Most measurements were made with the narrow spectral filter. This selects for the collective mode HRS signal, which is expected to be spectrally narrower than the individual molecule and solvent HRS signals, and also eliminates any two-photon fluorescence (2PF) contribution. Previous measurements of the PNA HRS spectrum found negligible 2PF,[15] and a scan of the VV HRS spectrum of the highest concentration PNA sample in the present work gives an upper bound of 0.4% for the 2PF contribution to the HRS signal for 60 cm^{-1} spectral bandwidth.

Solutions of PNA [$NO_2C_6H_4NH_2$] in acetone-d6 [$(CD_3)_2CO$] were made by mass, and the PNA concentration at $T = 25$ °C was calculated assuming volume additivity, using the density (0.868 g/mL) of acetone-d6,[16] and the extrapolated density (1.315 g/mL) of sub-cooled liquid PNA.[17] PNA (Chomophore Inc, long needle crystals) and acetone-d6 (Aldrich, 99.5 and 99.9 atom% D) were used as received. Samples were filled into the cell through a 0.2 μm particle filter. Absorption at the laser wavelength was small for the acetone-d6 solvent but not for the non-deuterated PNA

solute in the concentrated solutions. Measurements of the normalized HRS signal S_{VV}/P^2 as a function of laser beam power P were extrapolated to $P = 0$ to eliminate the effect of thermal defocusing of the laser beam by the sample. The HRS polarization ratios I_{VV}/I_{HV} and I_{HV}/I_{VH} were extrapolated to zero collection aperture as previously described, and I_{HV}/I_{VH} was corrected for ion contamination.[13] The narrow spike induced in the VH HRS spectrum by dissolved ions was measured by scanning the spectrum at 13 MHz resolution, and the ratio S/B of the integrated intensities for the spike (S) and the broader (B) intrinsic component of the VH HRS spectrum was determined. The corrected I_{HV}/I_{VH} polarization ratio is given by

$$(I_{HV}/I_{VH}) = (1 + S/B)(I_{HV}/I_{VH})_{meas}. \quad (1)$$

Figure 1 shows the VH spike in the high resolution VH HRS spectra for three PNA solutions. The spike is absent in the VV and HV HRS spectra.

Table I shows S_{VV}/P^2, S/B, I_{VV}/I_{HV}, and corrected I_{HV}/I_{VH} measured for neat acetone-d6 and PNA-acetone-d6 solutions with PNA concentration up to 1.6 mol/L (M). Also shown in Table I are the HRS polarization ratios with the solvent contribution subtracted, obtained using Eqs. (8)–(16) in Ref. 10. The PNA contribution dominates the HRS signal, so the PNA and solution values for the polarization ratios are negligibly different except at the lowest PNA concentrations. Figure 2 shows the concentration dependence of the PNA polarization ratios and the ion-induced signal. Orientation correlation of the PNA molecules is indicated by the deviation from $I_{HV}/I_{VH} = 1$ seen in Fig. 2(b), and this is the principal new observation from this work. This deviation is not apparent for the uncorrected I_{HV}/I_{VH} measurements since it is nearly cancelled by the opposite contribution from the VH spike. Measurements made on samples prepared using two different lots of acetone-d6 are represented by the open and filled circles in Fig. 2 (filled circles for the lot with higher, 99.99% purity). Although the ionic contamination and ion-induced signals are

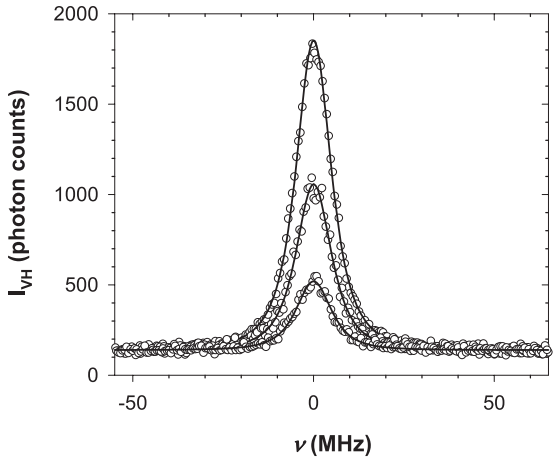

FIG. 1. High resolution scans of the VH HRS spectrum for three solutions with PNA concentration 0.241, 0.672, and 1.462 M, measured using the 0.3 cm^{-1} filter and normalized to the same integrated intensity for the broad background contribution. The solid curves fit to the data are the sum of a constant term and a term proportional to the instrument spectral response function. The integrated intensity of the spike increases with PNA concentration but the instrumentally broadened spike width is nearly constant (deconvolved width <1 MHz = 3×10^{-5} cm^{-1}).

TABLE I. HRS data for acetone-d6 solutions with PNA mole fraction x_{PNA} and number density ρ_{PNA}, measured with spectral bandwidth $\Delta\nu$. For each solution the normalized VV HRS signal S_{VV}/P^2 has been extrapolated to zero laser power, and the polarization ratios I_{VV}/I_{HV} and I_{HV}/I_{VH} have been extrapolated to zero collection aperture and corrected for the VH spike contribution $(S/B)_{VH}$. The polarization ratios for the PNA solute are obtained by subtracting the contribution of the solvent (see text). The relative uncertainty of S_{VV}/P^2 is ±10%.

x_{PNA} (%)	ρ_{PNA} (M)	$\Delta\nu$ (cm^{-1})	$\frac{S_{VV}}{P^2}$ (10^3 s^{-1} W^{-2})	$\left(\frac{S}{B}\right)_{VH}$ (%)	$\left(\frac{I_{VV}}{I_{HV}}\right)_{sol}$	$\left(\frac{I_{VV}}{I_{HV}}\right)_{PNA}$	$\left(\frac{I_{HV}}{I_{VH}}\right)_{sol}$	$\left(\frac{I_{HV}}{I_{VH}}\right)_{PNA}$
0	0	0.3	0.0024	12.2 ± 2.3	3.23 ± 0.07		0.603 ± 0.017	
0.081	0.011	0.3	0.279	4.7 ± 0.7	7.08 ± 0.08	7.15 ± 0.08	0.997 ± 0.011	1.010 ± 0.012
0.252	0.029	0.3	0.73	3.5 ± 0.4	7.22 ± 0.03	7.25 ± 0.03	1.015 ± 0.006	1.020 ± 0.006
0.413	0.056	0.3	1.44	3.4 ± 0.4	7.17 ± 0.06	7.18 ± 0.06	1.014 ± 0.008	1.017 ± 0.008
0.758	0.102	0.3	2.67	4.7 ± 0.3	7.16 ± 0.04	7.17 ± 0.04	1.045 ± 0.005	1.046 ± 0.005
1.10	0.148	0.3	3.93	5.2 ± 0.3	7.21 ± 0.02	7.21 ± 0.02	1.062 ± 0.006	1.063 ± 0.006
1.80	0.241	0.3	6.60	5.3 ± 0.2	7.20 ± 0.02	7.20 ± 0.02	1.083 ± 0.007	1.083 ± 0.007
2.99	0.400	0.3	11.5	11.9 ± 0.3	7.25 ± 0.03	7.25 ± 0.03	1.140 ± 0.007	1.141 ± 0.007
5.07	0.672	0.3	21.0	12.9 ± 0.3	7.31 ± 0.02	7.31 ± 0.02	1.218 ± 0.004	1.219 ± 0.004
7.70	1.009	0.3	34.5	23.1 ± 0.6	7.42 ± 0.03	7.42 ± 0.03	1.275 ± 0.008	1.276 ± 0.008
11.31	1.462	0.3	55.9	24.0 ± 0.3	7.41 ± 0.01	7.41 ± 0.01	1.342 ± 0.004	1.343 ± 0.004
0	0	60	0.027	4.8 ± 0.3[a]	2.80 ± 0.01[a]		0.766 ± 0.003[a]	
0.252	0.029	60	2.20		4.78 ± 0.02	4.83 ± 0.02		
0.413	0.056	60	4.32		4.83 ± 0.01	4.85 ± 0.01		
1.10	0.148	60	11.5		4.91 ± 0.01	4.92 ± 0.01		
1.80	0.241	60	18.9		4.99 ± 0.01	5.00 ± 0.01		
2.40	0.321	60	25.3	2.5 ± 0.1			1.049 ± 0.002	1.049 ± 0.002
5.07	0.672	60	54.2		5.16 ± 0.01	5.16 ± 0.01		
6.32	0.833	60	67.9	4.4 ± 0.1			1.103 ± 0.002	1.103 ± 0.002
11.31	1.462	60	124		5.41 ± 0.02	5.41 ± 0.02		
12.63	1.623	60	140	8.9 ± 0.1			1.176 ± 0.002	1.176 ± 0.002

[a]Reference 8.

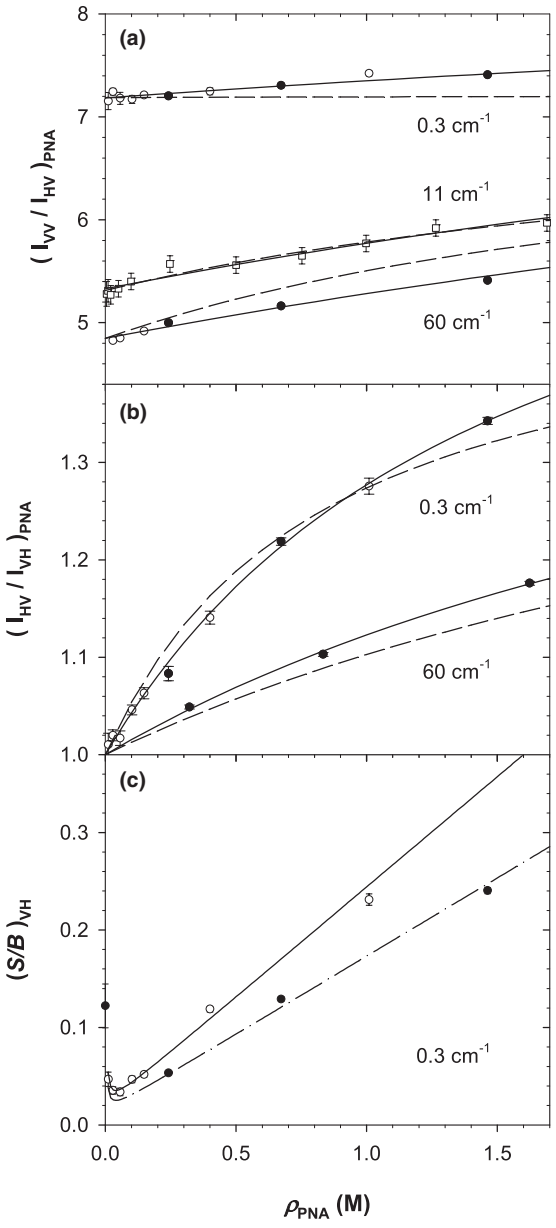

FIG. 2. (a) PNA concentration dependence of HRS polarization ratio I_{VV}/I_{HV} measured with 0.3, 11, and 60 cm^{-1} spectral bandwidth. The solid and dashed curves are Eqs. (17a) and (18a), respectively, fit to the data with the fit parameters given in Table II. The data for solutions prepared from two lots of acetone-d6 in this work are shown in (a), (b), and (c) as the filled circles (higher purity solvent, the solutions in Fig. 1) and open circles, while the 11 cm^{-1} data from Ref. 11 is shown as the open squares. (b) PNA concentration dependence of HRS polarization ratio I_{HV}/I_{VH} measured with 0.3 cm^{-1} and 60 cm^{-1} spectral bandwidth. The solid curves are the functions $1 + 0.70\rho_{PNA}/(\rho_{PNA} + 1.52\text{ M})$ and $1 + 0.55\rho_{PNA}/(\rho_{PNA} + 3.50\text{ M})$, while the dashed curves are Eq. (18b) fit to the data. (c) PNA concentration dependence of VH spike measured with 0.3 cm^{-1} spectral bandwidth. The solid and dashed-dotted curves are Eq. (10a) fit to the data (open and closed circles) for solutions prepared from two lots of acetone-d6 with different purity.

different for samples prepared from the two solvent lots, as shown in Fig. 2(c), all the corresponding corrected I_{HV}/I_{VH} data points fall on the same curve in Fig. 2(b).

The HRS signal will be analyzed in terms of four simultaneous contributions which are experimentally distinguished by their different spectral, polarization, and PNA concentration dependence. The first two contributions are from (1) uncorrelated molecules and (2) molecules with only short range correlations. Both contributions give $I_{HV}/I_{VH} = 1$, but different concentration dependence for I_{VV}/I_{HV}. The next two contributions are the result of long range molecular correlations, either (3) intrinsic to the liquid itself or (4) induced by dissolved ions. For (3) one finds $I_{HV}/I_{VH} \neq 1$, while for (4) the ratio $I_{HV}/I_{VH} = 0$ and the spectrum is 1000 × narrower. All four contributions are present both for neat acetone and for PNA solutions. The present analysis differs from the previous work by including the last two contributions.

III. ION-INDUCED HRS

The spike observed in the VH HRS spectrum is electric-field-induced second harmonic generation (ESHG) due to the electric field near dissolved ions orienting and distorting the molecules in the surrounding solution. The solution contains solvent molecules with concentration ρ_s, dissolved chromophores with concentration ρ_c, and ions of charge $\pm Ze$ and total concentration $\rho_i = \rho_+ + \rho_-$. The ion-induced spike intensity for the solution is[18]

$$S/B = (S/B)_\infty \frac{\rho_i/\rho_D}{1 + \rho_i/\rho_D}, \tag{2}$$

where ρ_D is the total ion concentration at which the Debye-Huckel screening parameter equals the scattering wavevector, $K_D = K$, given by

$$\rho_D = \frac{K^2 \varepsilon_0 \varepsilon_s k_B T}{Z^2 e^2}, \tag{3}$$

and the limiting intensity is

$$(S/B)_\infty = \frac{f(0)^2 k_B T}{2\varepsilon_0 \varepsilon_s} \frac{[\rho_s \Gamma_{s,\perp} + \rho_c \Gamma_{c,\perp}]^2}{\rho_s \langle \beta^2_{XZZ} \rangle_s + \rho_c \langle \beta^2_{XZZ} \rangle_c}. \tag{4}$$

The mean square lab frame hyperpolarizability $\langle \beta^2_{XZZ} \rangle$ gives the VH HRS intensity for randomly oriented molecules. The effective hyperpolarizability Γ for ESHG

$$\Gamma = \gamma + \mu^{(0)} \beta / 3 k_B T \tag{5}$$

has an intrinsic third-order contribution γ and a first hyperpolarizability β contribution due to orientation of dipolar molecules in the static ion electric field. The static local field factor $f(0)$ is

$$f(0) = \frac{\varepsilon_s (\varepsilon_\infty + 2)}{\varepsilon_\infty + 2\varepsilon_s}, \tag{6}$$

where ε_s and ε_∞ are the static and high frequency relative permittivity of the solution. Using the values $\varepsilon_s = 20.7$ and $\varepsilon_\infty = n^2 = 1.836$ for the pure solvent,[19] one obtains $f(0) = 1.837$ and $f(0)^2/\varepsilon_s = 0.1629$.

Several approximations are made to evaluate Eq. (4) using available data. Assuming Kleinman symmetry gives[20]

$$\beta_\parallel = 3\beta_\perp = \tfrac{3}{5} \sum\nolimits_\xi \beta_{z\xi\xi}, \tag{7a}$$

$$\gamma_\parallel = 3\gamma_\perp = \tfrac{1}{5} \sum\nolimits_{\xi\eta} \gamma_{\xi\xi\eta\eta}. \tag{7b}$$

A second good approximation for these highly dipolar molecules ($\mu^{(0)} = 6.87$ D for PNA[21] and 2.88 D for acetone[19])

is to neglect the γ contribution to Γ in Eq. (5). Based on gas phase hyperpolarizability measurements for PNA and acetonitrile,[22] one estimates $3k_BT\gamma/\mu^{(0)}\beta < 0.01$ for PNA and <0.1 for acetone. A final, more severe (one-dimensional, 1D) approximation is to assume that β_{zzz} is the only non-vanishing molecular hyperpolarizability component for these molecules. With the 1D approximation

$$\beta_\perp = \beta_{zzz}/5, \tag{8a}$$

$$\langle\beta^2_{XZZ}\rangle = (\beta_{zzz})^2/35, \tag{8b}$$

$$\langle\beta^2_{ZZZ}\rangle/\langle\beta^2_{XZZ}\rangle = I_{VV}/I_{HV} = 5. \tag{8c}$$

The measured polarization ratios for PNA and gas phase acetone[23] are consistent with Eq. (8c) and the 1D approximation, but $I_{VV}/I_{HV} \approx 3$ measured for liquid acetone-d6 indicates a significant additional intermolecular HRS contribution. The deviation from the assumed polarization ratio for the pure solvent can be accounted for by a factor $(1/5)(I_{VV}/I_{HV})$. With these approximations Eq. (4) for pure solvent becomes

$$(S/B)_\infty = \frac{1}{5}\left[\frac{I_{VV}}{I_{HV}}\right]\frac{7}{90}\frac{f(0)^2}{\varepsilon_s}\frac{[\mu_s^{(0)}]^2}{\varepsilon_0 k_B T}\rho_s. \tag{9}$$

For the PNA solutions, where the solvent HRS contribution is negligible, Eq. (4) becomes

$$(S/B)_\infty = A[\rho_c + 2C + C^2/\rho_c], \tag{10a}$$

where

$$A = \frac{7}{90}\frac{f(0)^2}{\varepsilon_s}\frac{\left[\mu_c^{(0)}\right]^2}{\varepsilon_0 k_B T}, \tag{10b}$$

$$C = \rho_s\frac{[\mu^{(0)}\beta_{zzz}]_s^2}{[\mu^{(0)}\beta_{zzz}]_c^2}. \tag{10c}$$

In this experiment the scattering wavevector is $K = 2\pi/\Lambda$ where $\Lambda \approx \lambda_0/(2n\sqrt{2}) = 279$ nm, and Eq. (3) gives $\rho_D = 25\ \mu$M for singly charged ions. Thus, the limiting value for *S*/*B* will be reached as a result of an ionized impurity A^+B^- at the 10^{-6} mole fraction level in the acetone solvent. Equation (9) predicts $(S/B)_\infty = 0.17$ for acetone ($\rho_s = 13.6$ M) at $T = 298$ K. Using Eq. (2) with $(S/B)_\infty = 0.17$, the value $S/B = 0.048 \pm 0.003$ measured for acetone-d6 with 60 cm^{-1} spectral bandwidth (see Table I) gives $\rho_i/\rho_D = 0.4$ and impurity concentration $\rho_i/2 = 5\ \mu$M, while the value $S/B = 0.122 \pm 0.023$ for the higher purity acetone-d6 sample measured with 0.3 cm^{-1} spectral bandwidth (which includes the entire spike but only 9% of the broad HRS component) gives $\rho_i/\rho_D = 0.07$ and $\rho_i/2 = 1\ \mu$M.

Figure 2(c) shows functions with the form of Eq. (10a) fit to *S*/*B* for PNA solutions measured with 0.3 cm^{-1} bandwidth, with fit parameters A' and C, where $A' = A(\rho_i/\rho_D)/(1 + \rho_i/\rho_D)$, ρ_i/ρ_D is assumed constant, and $A = 0.37$ M^{-1} is estimated using Eq. (10b) and accounting for the observation that only 30% of the broad PNA HRS spectrum falls within the 0.3 cm^{-1} bandwidth. The fit parameter $C = 0.039 \pm 0.005$ M is close to the value $C = 0.029$ M estimated from Eq. (10c), using the ratio of molecular hyperpolarizabilities $\beta_c/\beta_s = 200$ for PNA and acetone-d6 obtained from the VV HRS intensities in Table I measured with 60 cm^{-1} bandwidth. The *S*/*B* data in Fig. 2(c) for solutions prepared using two different lots of acetone-d6 are fit by separate curves, with fit parameter $A' = 0.23 \pm 0.01$ M^{-1} for the first curve, from which one estimates $\rho_i/\rho_D = 1.6$ and $\rho_i/2 = 20\ \mu$M, and $A' = 0.16 \pm 0.01$ M^{-1} for the second curve, from which one estimates $\rho_i/\rho_D = 0.8$ and $\rho_i/2 = 10\ \mu$M.

The observed intensity of the VH spike for the PNA solutions is close to the predicted limiting intensity, and is consistent with contamination by up to 20 μM of ionic impurities occurring during preparation of the 1 mL solution samples. Such ionic impurities in polar liquids are difficult to remove, and can be detected by the increase in the electrical conductivity of the solution.[24] The measured conductivities for the four samples shown by the filled circles in Figure 2(c) are 0.4 μS/cm for the neat acetone-d6, and 0.9, 0.9, and 1.3 μS/cm for the 0.241, 0.672, and 1.462 M PNA solutions. Using the typical limiting molar conductivity 183 S cm^2 mol^{-1} measured for Bu_4NPF_6 dissolved in acetone,[25] one estimates impurity concentrations 2 μM (versus 1 μM from HRS intensity) for the neat acetone-d6 sample, and 5, 5, and 7 μM (versus 10 μM from HRS intensity) for the PNA solutions. The ion concentrations estimated from the electrical conductivity and from the HRS spike intensity agree within the factor of two uncertainty of the comparison.

The VH HRS spike is an instructive example of a longitudinal polar mode since it is due to known orientation correlations for dipolar molecules in the radial electric field around an ion. At low ion concentration the ion is unscreened and the mean orientation of dipoles along the field direction is

$$\langle\hat{r}\cdot\hat{\mu}^{(0)}\rangle = f(0)\frac{\mu^{(0)}}{3k_BT}\frac{Ze}{4\pi\varepsilon_0\varepsilon_s}r^{-2}. \tag{11}$$

Equation (11) is plotted in Figure 3, showing the r^{-2} variation of the mean orientation for PNA molecules in acetone solution near a singly charged ion. The VH HRS spike intensity due to coherent scattering from the oriented molecules is proportional to the square of the volume integral

$$(K/4\pi)\int\int\int dV r^{-2}\cos\theta\sin(Kr\cos\theta) = \int_0^\infty dKr\, j_1(Kr) = 1, \tag{12}$$

where the scattering wavevector $\vec{K}$ defines the polar axis of the coordinates, $\cos\theta$ gives the projection of radial molecular dipoles onto $\vec{K}$, $\sin(Kr\cos\theta)$ accounts for phase differences between the second harmonic light scattered by molecules at different positions in the scattering volume, and $j_1(x) = (\sin x - x\cos x)/x^2$ is the spherical Bessel function of first order. Figure 3 shows the square of the integral in Eq. (12) as a function of the upper limit of the *r*-integration. One sees that the main contribution to the VH spike is coherent scattering from molecules with mean radial orientation $< 3 \times 10^{-5}$ at distances > 100 nm from the ion. HRS from molecules with such long range radial polar correlations gives $I_{HV}/I_{VH} < 1$. Note that translational symmetry is broken since the strength

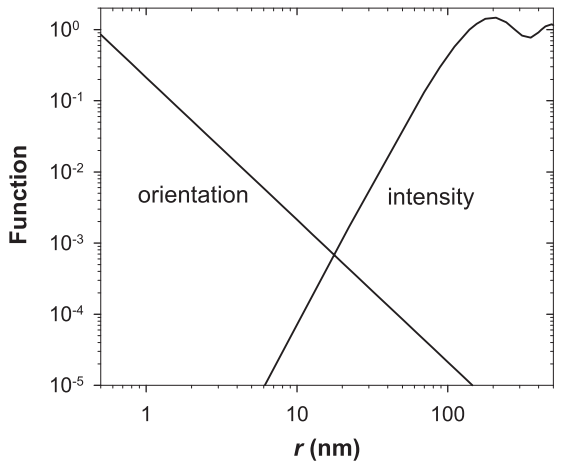

FIG. 3. Ion-induced correlation and VH HRS spike intensity as functions of distance r from the ion. The mean orientation of PNA molecules due to the electric field of a dissolved ion is given by Eq. (11) and decreases as r^{-2}. The coherent HRS intensity for PNA molecules within a spherical integration volume of radius r is given by the square of Eq. (12), which varies as r^4 initially and reaches its limiting value for $r > 100$ nm. Most of the VH spike intensity is due to molecules with mean orientation $<10^{-4}$.

of the intermolecular orientation correlation depends on position with respect to the ion, so the correlation between the PNA molecules is not described by a molecular pair correlation function.

IV. DIRECT DIPOLE-DIPOLE CORRELATION

Figure 2(a) shows that I_{VV}/I_{HV} increases with PNA concentration, and this observation was previously explained in terms of short range dipole-dipole correlations between the PNA molecules.[11] The coherent HRS contribution per molecule due to directly correlated pairs of 1D chromophores, given by Eqs. (4) –(6) of Ref. 11, is

$$\left\langle \beta^2_{ZZZ} \right\rangle_{coh} = 9 \left\langle \beta^2_{XZZ} \right\rangle_{coh} = 9\rho_c \beta^2_{zzz} I_{12}, \tag{13}$$

where

$$I_{12} = (12\pi)^{-2} \int \exp[-V(\vec{r}, \vec{\Omega}_1, \vec{\Omega}_2)/k_B T] \times \cos^3\theta_1 \sin\theta_1 d\theta_1 d\phi_1 \cos^3\theta_2 \sin\theta_2 d\theta_2 d\phi_2 r^2 \times \sin\theta_r dr d\theta_r d\phi_r \tag{14}$$

and $V(\vec{r}, \vec{\Omega}_1, \vec{\Omega}_2)$ is the unscreened dipolar hard-sphere interaction potential

$$V(\vec{r}, \vec{\Omega}_1, \vec{\Omega}_2) = \frac{(\mu_c^{(0)})^2}{4\pi\varepsilon_0 r^3}[(\hat{z}_1 \cdot \hat{z}_2) - 3(\hat{z}_1 \cdot \hat{r})(\hat{z}_2 \cdot \hat{r})] \text{ for } r > d, \quad = \infty \text{ for } r \le d, \tag{15}$$

where $\hat{z}_1$ and $\hat{z}_2$ are unit vectors along the polar axes of molecules 1 and 2, and $\vec{r}$ is the relative position vector. The integral I_{12} is a strong function of the hard sphere diameter d and the dimensionless interaction strength at closest approach $\eta = (\mu_c^{(0)})^2/(4\pi\varepsilon_0 d^3 k_B T)$. For $T = 298$ K and $\mu_c^{(0)} = 6.87$ D one obtains $\eta = 2.33$ and $I_{12} = 5.9 \times 10^{-3}$ nm^3 for $d = 0.79$ nm, and $I_{12} \propto d^{-8.5}$ over the range 0.75 nm $< d <$ 0.95 nm. The intermolecular distance and HRS intensity fluctuate as the molecules move and collide, and the time scale for these fluctuations determines the spectral width ν_2 of the coherent HRS contribution.

The incoherent HRS contribution can be expressed in terms of the molecular β tensor, which is the direct sum $\beta = \beta^{(1)} \oplus \beta^{(3)}$ of irreducible spherical tensors of first and third rank.[3] The spectrum for incoherent HRS from orientationally diffusing molecules will have a narrow component with width ν_1 and $I_{VV}/I_{HV} = 9$ due to $\beta^{(1)}$, and a wide component with width ν_3 and $I_{VV}/I_{HV} = 3/2$ due to $\beta^{(3)}$. For a 1D chromophore one has[3]

$$\left\langle \beta^2_{ZZZ} \right\rangle_{incoh} = \frac{9}{45}|\beta^{(1)}|^2 + \frac{6}{105}|\beta^{(3)}|^2 = \frac{9}{75}\beta^2_{zzz} + \frac{12}{525}\beta^2_{zzz} = \frac{1}{7}\beta^2_{zzz}, \tag{16a}$$

$$\left\langle \beta^2_{XZZ} \right\rangle_{incoh} = \frac{1}{45}|\beta^{(1)}|^2 + \frac{4}{105}|\beta^{(3)}|^2 = \frac{1}{75}\beta^2_{zzz} + \frac{8}{525}\beta^2_{zzz} = \frac{1}{35}\beta^2_{zzz}. \tag{16b}$$

The observed relative intensities due to the $\beta^{(1)}$ and $\beta^{(3)}$ contributions for PNA will differ from Eq. (16) because PNA is not exactly a 1D chromophore, and also because different fractions of the $\beta^{(1)}$ and $\beta^{(3)}$ spectra will fall inside the measurement bandwidth $\Delta\nu$.

Combining incoherent and coherent contributions from Eqs. (16) and (13) gives

$$\frac{I_{VV}}{I_{HV}} = \frac{9 + (12/7)A_1 + 9B_1\rho_c}{1 + (8/7)A_1 + B_1\rho_c}, \tag{17a}$$

$$B_1 = 75 T_2(\Delta\nu) I_{12}. \tag{17b}$$

The non-vanishing off-diagonal tensor components of β and the relative transmission of the three spectral components are accounted for in the factors A_1 and B_1. Fitting Eq. (17a) to I_{VV}/I_{HV} as a function of ρ_{PNA} gives the solid curves shown in Figure 2(a) and the values A_1, B_1, and I_{12} in Table II. The $\rho_{PNA} = 0$ limit of the I_{VV}/I_{HV} data for each bandwidth $\Delta\nu$ determines the value for the parameter A_1, and the change with PNA concentration determines B_1. The value $I_{12} = 5.9 \times 10^{-3}$ nm^3 is obtained using Eq. (17b) assuming that the coherent HRS spectrum is fully transmitted for $\Delta\nu = 60$ and 11 cm^{-1}, and $T_2(\Delta\nu) = 0.5$ for $\Delta\nu = 0.3$ cm^{-1}. The variation of A_1 and B_1 with $\Delta\nu$ seen in Table II indicates $\nu_1 < \nu_2 < \nu_3$, and $\nu_3 \approx 6$ cm^{-1} ($\nu_3/\nu_1 = 6$ is predicted for HRS from a spherical rotor[3]).

From the experimentally determined value $I_{12} = 5.9 \times 10^{-3}$ nm^3 one obtains the hard sphere diameter $d = 0.79$ nm assuming $\mu_c^{(0)} = 6.87$ D, or $d = 0.74$ nm using the previously assumed value $\mu_c^{(0)} = 6.2$ D (in agreement with $d = 0.73$ nm obtained in the previous work[11]). These hard sphere diameters have plausible values near the 0.67 nm length of the PNA molecule.[11] But these calculations neglect dielectric screening which reduces the interaction strength by the factor $f(0)/\varepsilon_s = 0.089$, and would result in negligible direct dipole-dipole correlations for $d > 0.7$ nm. One may argue that

TABLE II. Parameter values for fits of Eqs. (17a), (18a), and (18b) to $(I_{VV}/I_{HV})_{PNA}$ and $(I_{HV}/I_{VH})_{PNA}$ data from Table I and I_{VV}/I_{HV} data from Ref. 11.

$\Delta\nu$ (cm^{-1})	A_1	B_1 (M^{-1})	I_{12} (10^{-3} nm^3)	B_2 (M^{-1})	I_T (10^{-3} nm^3)
0.3	0.279 ± 0.004	0.133 ± 0.016	5.9 ± 0.5	2.40 ± 0.23	22.5
11[a]	0.839 ± 0.012	0.269 ± 0.023	5.9 ± 0.5	0.66 ± 0.06	6.1
60	1.086 ± 0.011	0.262 ± 0.024	5.9 ± 0.5	0.87 ± 0.11	8.1

[a]Reference 11.

dielectric screening is negligible since the main contribution to I_{12} is due to interactions at $r < 1$ nm during close molecular collisions, but for these close collisions the steric interactions are also strong and may over-ride the direct dipole-dipole interaction. Direct short range dipole-dipole correlations can account for the observed PNA concentration dependence for I_{VV}/I_{HV} if dielectric screening and the effects of steric interactions can be neglected. However, direct dipole-dipole correlations cannot account for any of the deviations from $I_{HV}/I_{VH} = 1$ seen in Table I and Figure 2(b).

V. LONG RANGE ORIENTATION CORRELATION

Departures from $I_{HV}/I_{VH} = 1$ will result from molecular orientation correlations in the form of longitudinal or transverse polar collective modes, with $I_{HV}/I_{VH} = 0$ for longitudinal polar modes and $I_{HV}/I_{VH} = 2$ for transverse polar modes.[14] The ion-induced orientation of solution molecules that gives the VH spike is an example of a long range longitudinal polar mode.[18] Deviations from $I_{HV}/I_{VH} = 1$ have also been observed in several pure liquids, indicating HRS contributions from longitudinal or transverse polar modes, where the intrinsic long range correlations in these liquids are thought to result from the same short range steric interactions that produce molecular crystals.[8]

The present HRS measurements for PNA-acetone solutions were intended to probe the range of intermolecular correlations for the acetone solvent by studying I_{HV}/I_{VH} as the distance between the PNA probe molecules was varied. However, it appears that the PNA molecules are not simply reporting the solvent molecular correlations since the PNA correlation has a form different from that of the acetone molecules. For pure acetone a dominant longitudinal polar mode is indicated by the measured value $I_{HV}/I_{VH} < 1$, while a dominant transverse polar mode is indicated by $I_{HV}/I_{VH} > 1$ measured for PNA in solution (see Table I and Fig. 2(b)). Nevertheless, the deviation from $I_{HV}/I_{VH} = 1$ indicates correlations between the PNA molecules, and a lower bound on the range of the PNA correlations can be estimated from the plot in Figure 4. This plot of I_{HV}/I_{VH} as a function of $r_{av} = \rho_{PNA}^{-1/3}$, the average distance between PNA molecules, shows that the correlations are still significant at $r_{av} = 3$ nm.

Another estimate of the range and strength of the correlations uses a simple explicit model for the orientation distribution of the PNA molecules.[8] The model assumes spherical domains with radius r_0, where fraction F of the molecules point azimuthally (e.g., clockwise) around an axis through the center of the domain, and where the remaining $(1 - F)$ molecules are randomly oriented. It also assumes that the individual domains are randomly oriented, and that the molecular hyperpolarizability is 1D so that β_{zzz} is the only non-zero component of β. The fraction F can be interpreted as the local mean orientation $\langle \cos\theta_z \rangle$ of the polar molecular z axis. For this model (at $\theta = 90°$, for small values of the scaled domain radius $x_0 = Kr_0 = 2\pi r_0/\Lambda$) one obtains

$$\frac{I_{VV}}{I_{HV}} = \frac{9 + (12/7)A_2 + (72/10)B_2\rho_c}{1 + (8/7)A_2 + B_2\rho_c}, \tag{18a}$$

$$\frac{I_{HV}}{I_{VH}} = \frac{1 + (8/7)A_2 + B_2\rho_c}{1 + (8/7)A_2 + (2/3)B_2\rho_c}, \tag{18b}$$

where

$$B_2 = \frac{450}{7} T_2(\Delta\nu) I_T, \tag{18c}$$

$$I_T(F, x_0) = \frac{F^2}{1 - F} \frac{\Lambda^3}{8^5} x_0^5. \tag{18d}$$

The factor A_2 again accounts for non-vanishing off-diagonal tensor components of β and the relative transmission of the incoherent $\beta^{(1)}$ and $\beta^{(3)}$ contributions, and has the same values as A_1 obtained by fitting Eq. (17a) to I_{VV}/I_{HV}. The B_2 values in Table II are obtained for each $\Delta\nu$ by simultaneously fitting Eq. (18a) to I_{VV}/I_{HV} and Eq. (18b) to I_{HV}/I_{VH}, giving the dashed curves in Figs. 2(a) and 2(b). For $\Delta\nu = 11$ cm^{-1} where there is only I_{VV}/I_{HV} data, a good fit nearly identical to the result using Eq. (17a) is obtained. The fits to the 0.3 and 60 cm^{-1} data in Figs. 2(a) and 2(b) are poor, and the I_T values in Table II [obtained assuming $\Delta T_2(\Delta\nu) = 1$] vary from 0.006 to 0.023 nm^3. The domain radius $r_0 = 5.0$–6.5 nm

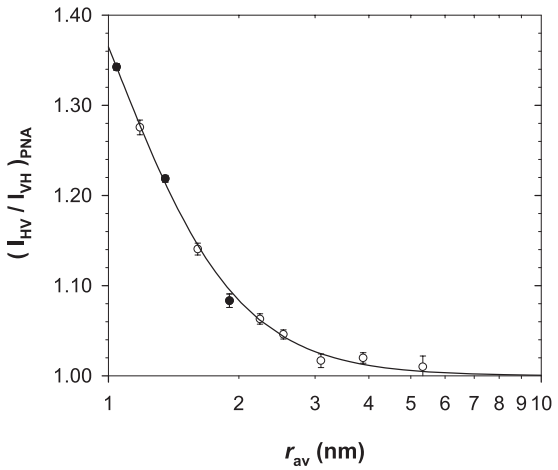

FIG. 4. HRS polarization ratio I_{HV}/I_{VH} as a function of $r_{av} = \rho_{PNA}^{-1/3}$, the mean distance between PNA molecules. The solid curve and the data points are the same as in Fig. 2(b) for $\Delta\nu = 0.3$ cm^{-1}.

is obtained from these I_T values using Eq. (18d) and assuming $F = 0.5$ for the correlated fraction of molecules, while the estimated domain radius increases to $r_0 = 14$–19 nm if $F = 0.05$ is assumed. This model indicates that strong correlations with a range near 10 nm are required to account for the HRS observations.

There are two main defects for the simple model which gives Eqs. (18a)–(18d). The model assumes that the strength and range of the orientation correlations are independent of PNA concentration, which may not be the case if the PNA correlations are not completely determined by the background solvent molecules. The assumed ideal experimental system is one where the probe and solvent molecules are similar in size and shape so that the probe reports but does not perturb the orientation correlations of the solvent molecules, and where the probe molecules have much higher nonlinearity so that HRS from the probe dominates the signal at all concentrations. The second defect of the simple model is that the assumed orientation correlation function may differ from the actual function. In Eqs. (18a) and (18b) the HRS polarization ratios for the correlated molecule contributions obtained from the simple model are $I_{VV}/I_{HV} = 7.2$ and $I_{HV}/I_{VH} = 3/2$, quite different from the respective values 9 and 2 for a pure transverse polar mode. However, a good fit to all the data is obtained if one sets $I_{VV}/I_{HV} = 7.5$ and $I_{HV}/I_{VH} = 5/3$ for the correlated molecule contributions, which suggests that the actual orientation correlation function is close to the assumed simple model and may be obtained by a small modification of the simple model.

VI. SUMMARY AND CONCLUSION

The concentration dependence of the HRS polarization ratios measured for PNA-acetone solutions gives information about the strength and range of molecular orientation correlations. The HRS observations were analyzed in terms of three contributions to the molecular correlations: (i) the ion-induced long range longitudinal polar mode due to radial oriented dipolar molecules, (ii) direct dipole-dipole correlations between the PNA molecules ignoring the solvent, and (iii) a long range transverse polar mode for PNA molecules tracking the orientation correlations of the acetone solvent molecules. The first contribution results in coherent HRS from domains with 100 nm radius around each dissolved ion and is clearly distinguished by the narrow spectrum it produces (<1 MHz due to diffusive ion motion). The second contribution can account for the concentration dependence of I_{VV}/I_{HV} if dielectric screening and steric effects are negligible for close molecular collisions, but cannot account for any deviation from $I_{HV}/I_{VH} = 1$. The third contribution was evaluated using a simple model and is in qualitative but not quantitative agreement with the HRS observations. Refinements of the model are suggested which may result in quantitative agreement with the measurements and lead to a better determination of the molecular correlations. Based on the simple model one estimates that strong orientation correlations ($F > 0.1$) exist over domains with 10 nm radius. Since the correlations depend on position in the domain, they break the translational symmetry of the liquid and cannot be expressed by a molecular pair correlation function.

ACKNOWLEDGMENTS

This work was supported by the National Science Foundation through Grant No. CHE-1212114.

[1] K. Clays and A. Persoons, Phys. Rev. Lett. **66**, 2980 (1991).
[2] R. Bersohn, Y. H. Pao, and H. L. Frisch, J. Chem. Phys. **45**, 3184 (1966).
[3] P. D. Maker, Phys. Rev. A **1**, 923 (1970).
[4] S. Kielich, Phys. Lett. A **27**, 307 (1968).
[5] S. Kielich, J. R. Lalanne, and F. B. Martin, Phys. Rev. Lett. **26**, 1295 (1971).
[6] P. Kaatz and D. P. Shelton, Mol. Phys. **88**, 683 (1996).
[7] D. P. Shelton, J. Chem. Phys. **132**, 154506 (2010).
[8] D. P. Shelton, J. Chem. Phys. **136**, 044503 (2012).
[9] J. Chen and K. Y. Wong, J. Chem. Phys. **122**, 174505 (2005).
[10] D. P. Shelton, J. Chem. Phys. **133**, 234507 (2010).
[11] Y. C. Chan and K. Y. Wong, J. Chem. Phys. **136**, 174514 (2012).
[12] D. P. Shelton, W. M. O'Donnell, and J. L. Norton, Rev. Sci. Instrum. **82**, 036103 (2011).
[13] D. P. Shelton, Rev. Sci. Instrum. **82**, 113103 (2011).
[14] D. P. Shelton, J. Opt. Soc. Am. B **17**, 2032 (2000).
[15] P. Kaatz and D. P. Shelton, J. Chem. Phys. **105**, 3918 (1996).
[16] J. Szydlowski, R. G. de Azevedo, L. P. N. Rebelo, J. M. S. S. Esperanca, and H. J. R. Guedes, J. Chem. Thermodyn. **37**, 671 (2005).
[17] F. Huyskens, H. Morissen, and P. Huyskens, J. Mol. Struct. **441**, 17 (1998).
[18] D. P. Shelton, J. Chem. Phys. **130**, 114501 (2009).
[19] *CRC Handbook of Chemistry and Physics*, 68th ed., edited by R. C. Weast (CRC, Boca Raton, 1987).
[20] D. P. Shelton and J. E. Rice, Chem. Rev. **94**, 3 (1994).
[21] F. Sim, S. Chin, M. Dupuis, and J. E. Rice, J. Phys. Chem. **97**, 1158 (1993).
[22] P. Kaatz, E. A. Donley, and D. P. Shelton, J. Chem. Phys. **108**, 849 (1998).
[23] D. P. Shelton, J. Chem. Phys. **137**, 044312 (2012).
[24] N. J. Felici, Br. J. Appl. Phys. **15**, 801 (1964).
[25] D. L. Goldfarb, M. P. Longinotti, and H. R. Corti, J. Solution Chem. **30**, 307 (2001).